Investigation of Gravitational Effects in Pulse Tube Cryocoolers Using 3-D CFD Simulations

T. Fang[1], T. I. Mulcahey[2], P.S. Spoor[3], M.D. Perrella[1], T. J. Conrad[4], S. M. Ghiaasiaan[1]

[1]Georgia Tech Cryo Lab, G.W. Woodruff School of Mechanical Engineering, Georgia Institute of Technology, Atlanta, GA 30332 USA

[2]CSA Medical Inc., Lexington, Massachusetts 02421

[3]Chart, Biomedical Division, Chart Inc., Troy, New York 12188

[4]Raytheon Space and Airborne Systems
El Segundo, CA 90245 USA

ABSTRACT

Stirling-type pulse tube cryocoolers (PTC) are increasingly used in tactical applications as well as ground testing of space systems. Some PTCs exhibit sensitivity to gravitational orientation and often lose significant cooling performance unless situated with the cold end pointing downward. Previous investigations have indicated that some coolers exhibit sensitivity while others do not; however, a reliable method of predicting the level of sensitivity during the design process has not been developed. In this study, we attempt to derive a semi-analytical method that can be used to ensure that a PTC will remain functional in adverse static tilt conditions. The development of the method is based on experimentally-validated 3-D computational fluid dynamics (CFD) simulations that identify relationships between pulse tube geometry and operating conditions including frequency, mass flow rate, pressure ratio, mass-pressure phase, hot and cold end temperatures, and static tilt angle. The validation of the computational model is based on experimental data related to a number of pulse tube cryocoolers. Simulation results and experimental data are gathered to yield the relationship between inclined PTC performance and pulse tube convection numbers (N_{PTC}). The data hereby can offer guideline for PTC designs.

INTRODUCTION

Stirling-type pulse tube cryocoolers (PTC) are especially attractive for some applications because of their mechanical simplicity and long life reliability. Pulse tubes are critical components of which the primary function is to create phase lag of mass flow to pressure wave. Many PTCs experience significant losses of cooling power when the cold end is not pointing downward due to convective effects occurring in the pulse tube [1-3]. This phenomenon has been experimentally and numerically studied. Swift and Backhaus [4, 5] experimentally analyzed gravity orientation

Cryocoolers 19, edited by S.D. Miller and R.G. Ross, Jr.

sensitivities of PTCs and analytically formulated a theory to explain the phenomenon and offer guidelines to PTC designs. Berryhill and Spoor [6] found that their experimental results generally agreed with Swift and Backhaus's [4, 5] theory. But their work suggests that the safety factor in the theory may need to be modified in order to ensure reliable inclined condition performance.

Meanwhile, computational fluid dynamics (CFD) approaches have been used to model pulse tube flow and thermal physics as well. Taylor [7, 8] developed a two-dimensional, axisymmetric CFD model as a predictive tool of PTC designs. Some 3-D PTC CFD simulation approaches have also been implemented and experimentally validated [9-11]. Some parametric studies have been conducted based on 3-D CFD models [12].

In this study, which is a follow-up to an earlier investigation [9, 12] based on more data and analysis, a half-symmetric 3-D CFD model is used in component level pulse tube parametric analysis. Simulation and experimental results are gathered to exhibit the relationship between inclined PTC performance and pulse tube convection numbers (N_{PTC}).

PULSE TUBE THERMODYNAMICS AND CONVECTIVE INSTABILITY

The thermodynamics and convective instability of pulse tubes are briefly reviewed in this section. More detail can be found in [9, 12]. The relevant energy flows, and their directions, are noted in Figure 1 and consistent with a cycle-averaged condition. In Figure 1, boundary planes one (1) and two (2) represent the cold and warm ends, respectively.

Pulse Tube Thermodynamics

The pulse tube converts the Gibbs free energy to an enthalpy flow (travels from cold to warm). The Gibbs energy, also referred as the acoustic (PV) power and is expressed as,

$$\left\langle P\dot{V}\right\rangle = \frac{1}{2}P_d\dot{V}_d\cos\left(\theta_{m-p}\right) \tag{1}$$

where P_d is the dynamic pressure amplitude, $V\acute{E}_d$ is the volume flow amplitude, and $\ddot{\imath}_{m\text{-}p}$ is the phase between mass flow and pressure. In an ideal pulse tube, the conversion is perfect and the enthalpy flow is equal to the Gibbs energy. In an ideal pulse tube with using the remaining terms in Figure 1, it can be shown that the total net energy flow in the pulse tube at a cyclic condition is,

$$\left\langle \dot{E}_{PT,net}\right\rangle = \left\langle \dot{H}\right\rangle - \left\langle \dot{Q}_g\right\rangle - \left\langle \dot{Q}_w\right\rangle \tag{2}$$

where $\left\langle \dot{H}\right\rangle$ is the pulse tube enthalpy flow, $\left\langle \dot{Q}_g\right\rangle$ is the conduction in the working fluid, and $\left\langle \dot{Q}_w\right\rangle$ is the conduction in the solid wall of the pulse tube. In practice, the acoustic power to enthalpy conversion is not perfect due to numerous complex loss mechanisms that include all forms of streaming, shuttle heat transport, turbulent mixing and jetting, and gravitationally induced instability. All these mechanisms reduce the available enthalpy flow in the pulse tube and subsequently the cooling power. Minimizing these losses has been the subject of numerous empirical and numerical studies over the years. The mechanisms responsible for all these losses are relatively well understood, with the exception of gravitationally-induced instability.

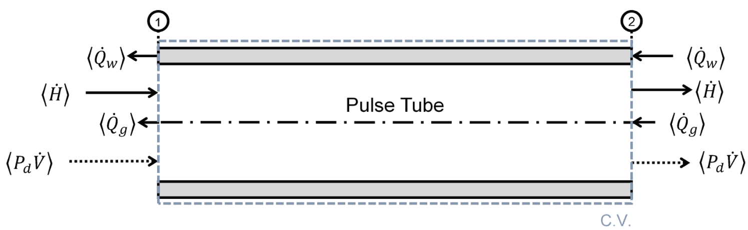

Figure 1. Illustration showing the relevant energy flows for a pulse tube. PV power is included in the energy flow diagram with dashed arrows for reference. The temperature gradient is cold to hot from left to right, i.e. from 1→2.

The gravitationally-induced stability loss in pulse tube coolers causes severe cooling power degradation when the pulse tube cryocooler is operated in a configuration where the temperature gradient (cold below warm) is not aligned with the gravitational field. Once the cooler deviates from the ideal gradient orientation with respect to gravity, the flow tends to become unstable, and an undesirable circulation cell develops when instability prevails.

In this work, we quantify the loss associated with the tilt effect as,

$$|L(\theta)| = \frac{\left\langle \dot{E}_{PT,net}(0)\right\rangle - \left\langle \dot{E}_{PT,net}(\theta)\right\rangle}{\left\langle \dot{E}_{PT,net}(0)\right\rangle} \tag{3}$$

where $\left\langle \dot{E}_{PT,net}(0)\right\rangle$ is the net pulse tube energy flow at zero degrees deviation from ideal and $\left\langle \dot{E}_{PT,net}(\theta)\right\rangle$ (i.e., when the cold tip is above the warm end of the cryocooler, and the axis of the cryocooler is vertical) is the net pulse tube energy flow at an angle θ removed from zero. A clear understanding of this loss and its parametric dependence on various design and operational parameters is required to enable the use of modern high-frequency pulse tube coolers in applications where operation under non-ideal cooler-gravitation alignment in expected.

Convective Instability

A classic example of convective instability arises in a quiescent enclosure initially containing quiescent fluid, in which the top and bottom surfaces are at differing temperatures and the vertical surfaces are adiabatic. For any specific no-trivial tilt angle at some critical temperature differential, the buoyant forces in the fluid overcome viscous forces and buoyncy-driven cells develop. The strength of these cells depends on the severity of the imbalance between buoyancy and viscous forces and is characterized using the Rayleigh number. The phenomenology of instability in a pulse tube is to some extent similar. In the pulse tube, unlike an otherwise quiescent fluid, there is a bulk velocity arising from the oscillating flow field. In this case the convection stability criteria can be related to a ratio of the inertial forces (and not viscous forces) in the oscillating fluid relative to the buoyant forces in the fluid.

The convective instability and conditions leading to its occurrence in pulse tube can of course be modeled using high-fidelity computational fluid dynamic (CFD) simulations, provided that such simulations are set up with correct boundary conditions and closure relations. Such CFD simulations are complex and computationally demanding given that they involve periodic multi-dimensional flow. Simpler, semi-analytical models suitable for iterative design and optimization calculations are thus needed.

Swift and Backhaus [4, 5] modeled the convective instability in a pulse tube based on an analogy with an inverted pendulum, noting that a statically unbalanced inverted pendulum can be dynamically stabilized using correct dynamic excitation at its base. This observation is consistent with experimental evidence related to high frequency pulse tube cryocoolers. Experiment has shown that increased operating frequency in pulse tube cryocoolers mitigates the convective instability caused by tilt from ideal vertical configuration. Using a semi-analytical model Swift and Backhaus [5] argued that the forthcoming non-dimensional pulse tube convection number could be used as a criterion to determine the vulnerability of a pulse tube cryocooler to the adverse effect of non-ideal tilt angle,

$$N_{PTC} = \frac{\omega^2 a^2}{g\left(\alpha_s D \sin\theta - L\cos\theta\right)}\sqrt{\left(\frac{\Delta T}{T_{avg}}\right)} \tag{4}$$

where ω is the angular frequency associated with the flow pulsation, α is the mass flow amplitude, g is gravitational acceleration, α_s is empirical fitting parameter, D and L are the pulse tube diameter and length, respectively, θ is the tilt angle from vertical, ΔT is the temperature difference between hot and cold, and T_{avg} is the average gas temperature in the pulse tube.

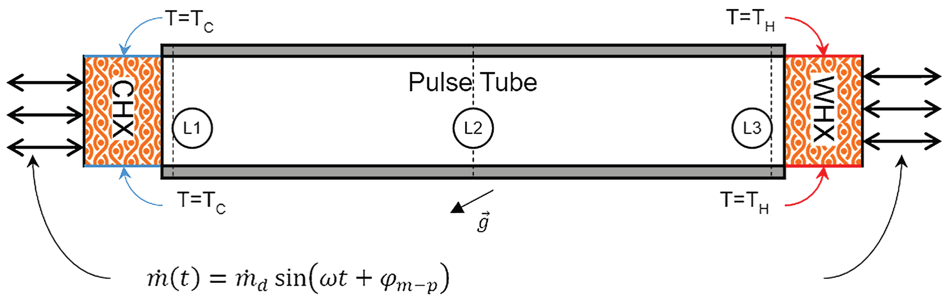

Figure 2. Schematic view of the computational domain along the plane of symmetry. Patterned sections represent porous domains. Solid filled wall section represents solid domain. Dashed lines represent computational monitor planes. Double headed arrows represent oscillatory boundary conditions.

Simulation Methods

A brief overview of the key characteristics of the ANSYS CFD [13] simulation methods used in this study will be given here. For further details of the simulation methods the reader is directed to [9], which describes two distinct methods for simulating the convective losses: a full-system approach which simulates an entire pulse tube cooler system, and an isolated model that includes only the pulse tube and adjacent heat exchangers. Figure 2 depicts an isolated system. The argument for the limitation of the simulation domain to the pulse tube and its adjacent heat exchangers is that these are the key components that are most sensitive to gravity. All simulations are performed in 3-D half-symmetry, with the symmetry plane coincident with the plane in which the gravity vector varies. It was shown earlier that an isolated model introduces only approximately 6% error to the predictions, while reducing the number of CPU's required for parallel processing by a factor of four and simultaneously reducing the simulation time by a factor of three. Validation of this model against a set of commercial cryocoolers is given in [10], where error was reported as a percentage of the net energy flow across the pulse tube. An average error of 3.7% and a maximum error of 8.2% were reported using this modeling methodology, with largest errors occurring when the cooler was driven below its design input power, resulting in very low Reynolds numbers and therefore was most unstable. Numerical simulation error magnitudes were in the range of approximately 100 mW, indicating that the simulation method is most aptly suited for pulse tube coolers with larger net cooling capacity.

An open system modeling method is used for the isolated domain consisting of the cold heat exchange (CHX), pulse tube, and warm heat exchanger (WHX) (See Figure 2.) A sinusoidal mass flow boundary condition with specified temperature, magnitude and phase angle relative to pressure oscillation is applied at the entrance to the CHX (the left side of the system shown in Fig. 2). A sinusoidal pressure with specified amplitude and frequency ω provides closure to the fluid domain at the warm heat exchangers. Isothermal boundary conditions are imposed at the cold and warm heat exchangers. Monitoring surfaces are defined across the pulse tube locations denoted L1, L2 and L3, which record the thermodynamic and hydrodynamic parameters required to compute and isolate energy flows across the domain. Conjugate heat transfer with the pulse tube wall is included to simulate thermally driven boundary phenomena that may impact off-axis performance. Gas properties are obtained from the NIST real gas models reported in the REFPROP database [14]. The heat exchangers are modeled as porous domains with hydrodynamic parameters based on those reported for packed screens in oscillatory flow [15].

The domain is spatially discretized using approximately 75,000 ordered mesh elements, the minimum quantity found to yield grid-independence with discretization error less than 0.5% of the net pulse tube energy flow. Inflation meshing was used within the fluid domain to capture boundary effects. The transient simulation was carried out to periodic steady state using time steps that yielded 400 samples per period of oscillation. Typical simulations required approximately 30,000 time steps for the solution to converge for convectively stable configurations. Simulations were carried out on high performance computing (HPC) cluster resources in order to compute the solution in

12 parallel processes, with a simulation duration of approximately 255 hours per case. In some instances 24 CPUs were used for each case, which reduced simulation time to 155 hours.

RESULTS

We examined 145 simulated pulse tube conditions with driving frequency ranging from 25 Hz to 60 Hz, cold end temperatures from 4 K to 80 K, rejection temperatures of 20 K to 300 K, mass flow rates from 1 g/s to 4 g/s, and mass flow phase angles of -30° to +30° relative to pressure. Two computational domains were used with length/diameter aspect ratio of eight (8), commonly used as a design minimum, and four (4), which is often required for larger capacity pulse tubes as cross-sectional area scales with mass flow while length does not. Experimentally measured off-axis performance for three commercial cryocoolers are also included in the analysis to add to the body of data from which to draw conclusions.

Upon completion, each simulation was post-processed to determine the net energy flow across the pulse tube at the cold end according to Equation 1, adjacent to the cold heat exchanger but within the gas domain outside the transition from porous to open flow channel. The energy flow data at varying inclination angle θ was compared to the energy flow in the vertical orientation via Equation 3, yielding the normalized energy flow loss |L|, for which a value of zero indicates no reduction in cooling performance at the specified angle, a value of one indicates complete loss of net cooling power, and a value greater than one indicates that the pulse transfers energy from the warm end to the cold end. Normalized energy flow loss is plotted in Figures 3, 4 and 5 as a function of the tilt angle, with the oscillatory Reynolds number Re^{δ} as a parameter. The Reynolds number based on Stokes' boundary layer thickness is used to characterize the flow and ranges from 43 (very laminar) to 350. The oscillatory Reynolds number at which transition to intermittent turbulence occurs is approximately 500 [16].

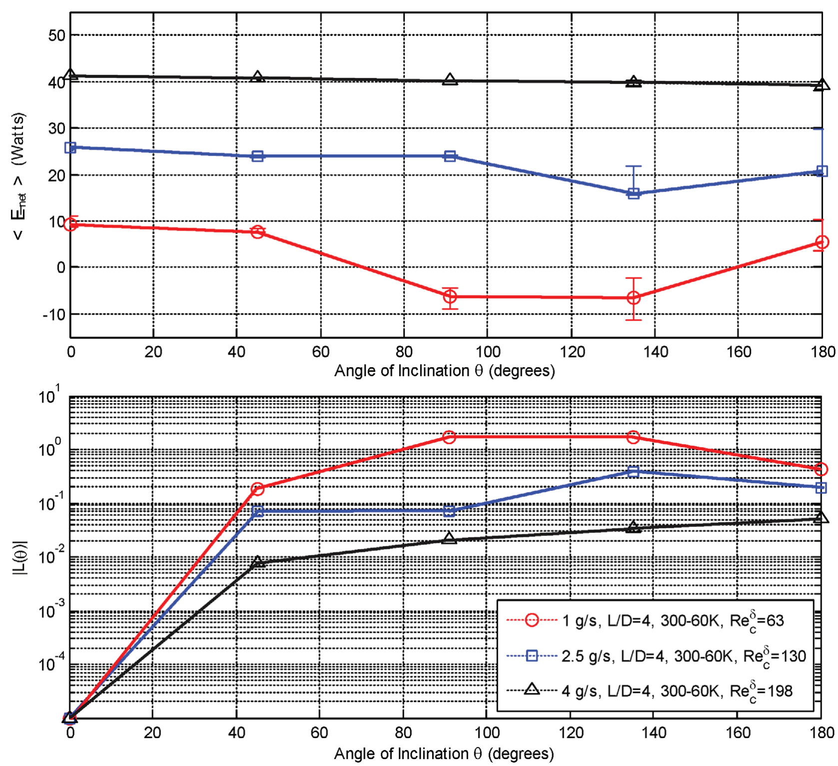

Figure 3. Net pulse tube energy flow and normalized loss coefficient for pulse tube with L/D=4 aspect ratio driven at 60 Hz at various mass flows in five discrete orientations with respect to gravity. Phase angle of -30° (mass lags pressure) and pressure ratio of 1.2 operating between 300 K and 60 K.

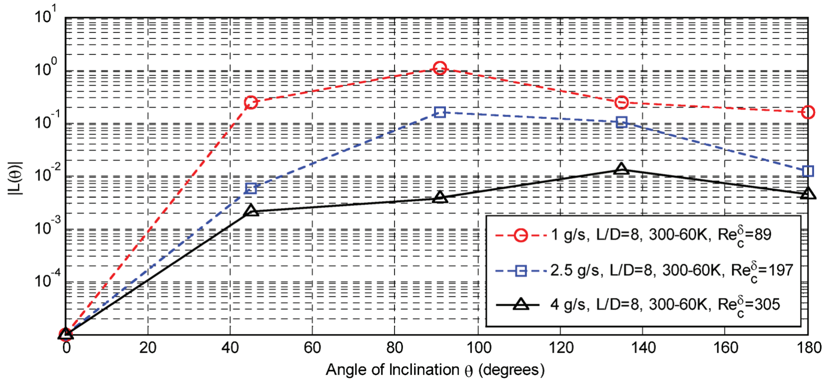

Figure 4. Net pulse tube energy flow and normalized loss coefficient for pulse tube with L/D=8 aspect ratio driven at 60 Hz at various mass flows in five discrete orientations with respect to gravity. Phase angle of -30° (mass lags pressure) and pressure ratio of 1.2 operating between 300 K and 60 K.

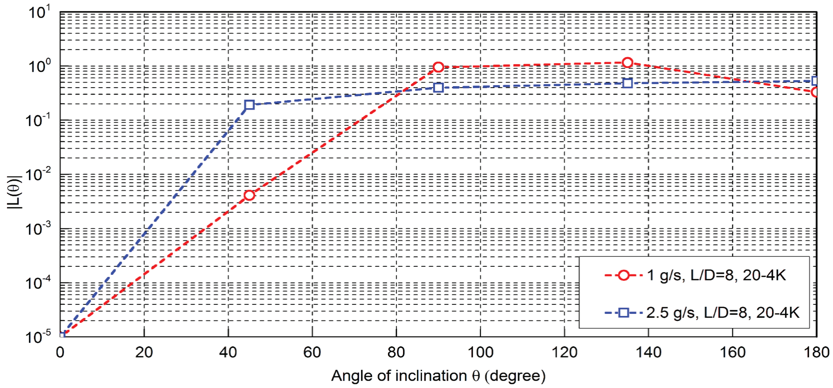

Figure 5. Net pulse tube energy flow and normalized loss coefficient for pulse tube with L/D=8 aspect ratio driven at 60 Hz at various mass flows in five discrete orientations with respect to gravity. Phase angle of -30° (mass lags pressure) and pressure ratio of 1.2 operating between 20 K and 4 K.

Figure 3 presents representative energy flow loss data as a function of the mass flow amplitude, and therefore the Reynolds number, for a pulse tube with length-to-diameter aspect ratio of four. The pressure used in all simulations was 2.0 MPa with a pressure amplitude of 400 kPa. The mass flow amplitude is directly related to the input power, and therefore the efficiency decreases significantly for higher mass flows at inclination angles above 45°. The error bars displayed in the net energy (4) under the typical pulse tube design condition that mass flow lags pressure by 30°. The average flow plots in Figures 3 and 4 are used for unstable cases to show the maximum and minimum energy flows observed over the final 0.25 s of simulated flow time. Larger error bars indicate a more unstable flow regime.

Figure 4 compares performance for a pulse tube with identical operating conditions to the results reported in Figure 3 and identical pulse tube gas volume but with an aspect ratio of eight (8). In this case, only a single operating point (1 g/s, 90° orientation) resulted in catastrophic loss of cooling, and an increase in the mass flow rate to 4 g/s reduced orientation sensitivity by two orders of magnitude.

Figure 5 shows normalized cooling of the pulse tube in the same working condition as shown in Fig. 4, except the pulse tube cryocooler operates between 20 K and 4 K. In this case, the performance of the pulse tube was more sensitive to gravity orientation than when the pulse tube operated between 300 K and 60 K temperatures. Two points (1 g/s, 90° and 135° orientation) shown catastrophic loss of cooling. Other points also presented more loss of cooling in comparison with Fig. 4.

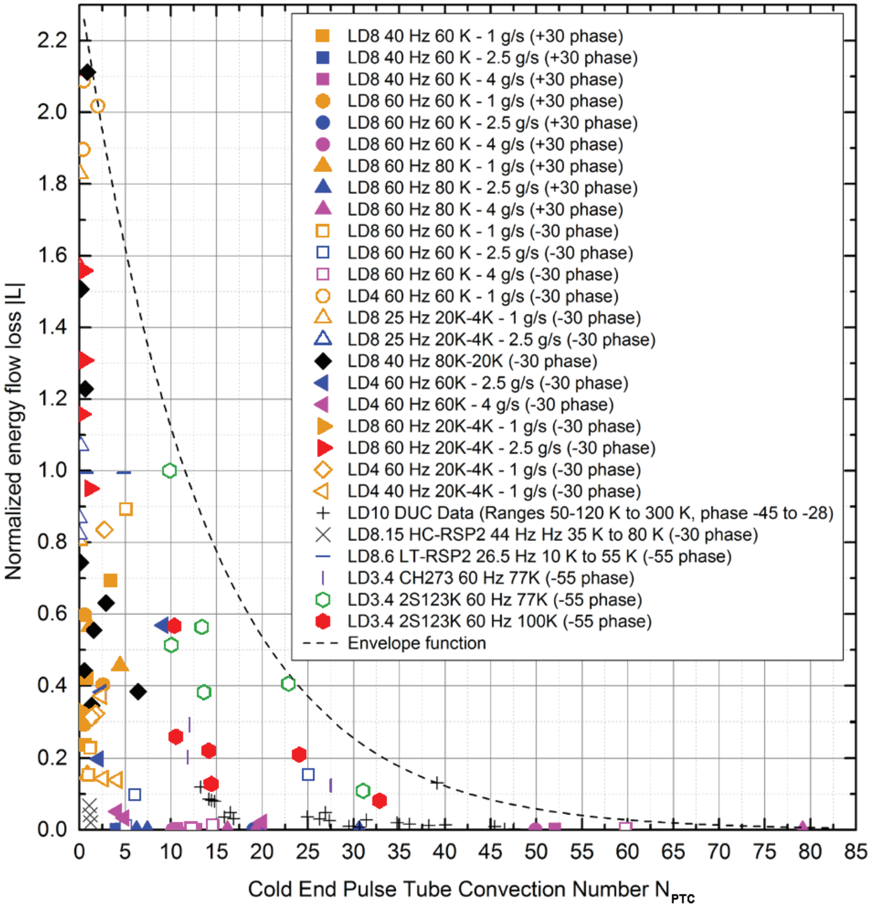

Figure 6. |L| vs N_{PTC} results. Legend entries indicate the aspect ratio (LD), driving frequency, cold end temperature, mass flow, and phase angle of mass flow relative to pressure (dash line indicates the envelop function).

In extreme low temperatures (in this case 20 K to 4 K), inclination effects are more severe because of the stronger convection resulted from larger variances in density.

In order to assimilate all data sets collected, the pulse tube convection number N_{PTC} defined by Equation 4 was computed for each case. Figure 6 shows the normalized energy flow loss |L| as a function of the computed pulse tube convection number N_{PTC} for all numerically simulated and experimentally measured data collected in this study. There is considerable scatter in the data depicted in Figure 6. This is understandable in view of the simplicity of the model and the complexity of the thermo-fluid phenomena in a pulse tube. Thus, the pulse tube convection number should only be used as an order of magnitude indicator of the orientation sensitivity. The calculation of the expected loss in energy flow of a pulse tube cryocooler may need a detailed CFD simulation.

The convective flow patterns can be qualitatively different for different conditions and N_{PTC} may not be able to fully characterize a coolers' performance. Figure 7 compares the flow patterns at different inclination angles. The sample case had the parameters of LD8, 60 Hz, 1 g/s mass flow, -30° phase lag of mass to pressure, and warm and cold heat exchanger temperatures of 20 K and 4 K, respectively. The temperature gradients in the middle part of the pulse tube indicated clear convective flow patterns for 90°, 135° and 180° conditions. However, the patterns were not the same at different angles, even in terms of their overall structure. Figure 8 depicts the convective flow patterns for 90° and 180° tilt angles. Contours of several time steps within a cooling cycle are shown in

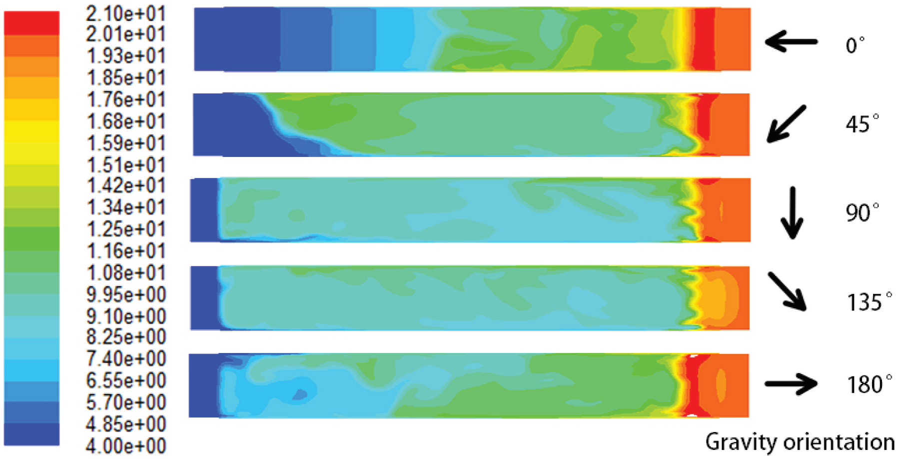

Figure 7. Sample temperature contours (LD8, 60 Hz, 1 g/s, 20K-4K, -30 phase) at inclination angle of 0, 45, 90, 135 and 180 degrees.

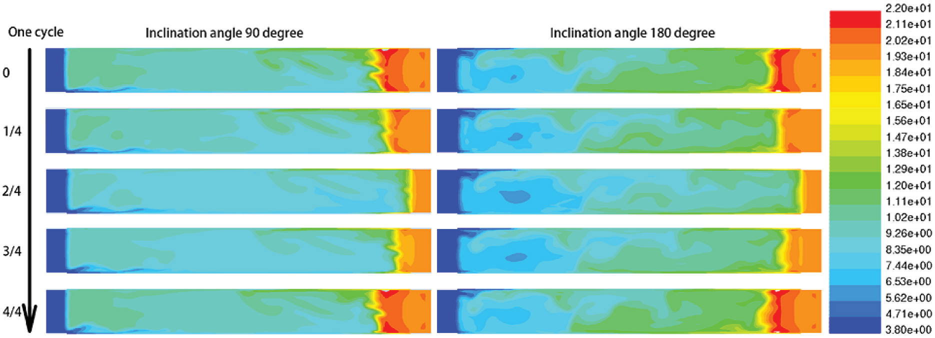

Figure 8. Temperature contours (LD8, 60 Hz, 1 g/s, 20K-4K, -30 phase) of 90 and 180 degrees inclination angle at 0/4, 1/4, 2/4, 3/4 and 4/4 point of a full cooling cycle.

this figure. Flow patterns for the same cases were shown in Fig. 7. At 90° inclination, there was a strong convective circulation that persisted during the entire cooling cycle and could not be broke down by oscillation. On the other hand, the convective flow inside the pulse tube at 180° is chaotic, indicating no clear flow circulation pattern, and instead suggests relatively localized mixing near the warm end of the pulse tube. Convective flow was not traveling from one end of the pulse tube to the other end, as could be observed in the case of 90° tilt, for example. As a result, the thermal stratification at 180° tilt angle was better than the thermal stratification at 90° tilt angle, which implied weaker undesirable convective heat transfer at 180° tilt angle. As a result, as noted in Figs. 3, 4 and 5, the 180° cases generally had a smaller cooling loss than the 90° case, even though N_{PTC} at 180° is smaller than at 90°.

DISCUSSION

In general, observation of the data presented in Figure 6 yields interesting trends. There is notable evidence that use of higher operating frequency, when possible, is advisable. Furthermore, larger aspect ratio pulse tubes generally perform better off-axis for temperatures above ~60 K. For temperatures below ~15 K, off-axis effects are noticeably more severe as expected due to the larger disparity in density between cold and warm ends when compared to more moderate temperature cases. Finally, larger mass flow amplitudes generally serve to reduce the off-axis sensitivity. This is attributed to larger inertial forces, which are stabilizing when compared to the buoyancy forces.

All of the observed cases reported in Figure 6 report orientation sensitivity in terms of normalized energy flow loss below a bounding function which is fitted to the largest observed loss in over the full range studied. These extreme points are fitted with an exponential decay function of the form shown in Equation 5. All points simulated and measured fall below the cutoff line described by Equation 5.

$$|L(\theta)|_{max} \leq 2.3446e^{-0.0738N_{PTC}} \tag{5}$$

The utility of the data reported herein is the ability to determine the expected order of magnitude loss as a function of a calculated pulse tube convection number for a given theoretical design. This factor can be incorporated in a scoping level study to avoid designs that indicate undesirable orientation sensitivity. Once a prospective design is developed, it should be examined using the above described 3-D CFD methodology at the worst anticipated angle of inclination to verify the level of sensitivity prior to fabrication.

CONCLUSIONS

Three-dimensional CFD simulation has been successfully applied to predict performance losses due to gravity-driven convective instability in pulse tube cryocoolers over a wide range of operating characteristics and two geometries. The results were characterized in terms of a nondimensional loss of net energy flow as well as the nondimensional pulse tube convection number. The results indicate that the upper limit of the magnitude of cooling power loss decays exponentially with increasing pulse tube convection number and sensitivity is minimized by applying the design which yields the highest laminar Reynolds number in the pulse tube. The reported relationship in this article should be used for scoping purposes only. Complete thermodynamic designs should rely on detailed 3-D CFD-assisted simulations using correct boundary conditions and closure relations.

REFERENCES

1. Thummes, G., M. Schreiber, R. Landgraf, and C. Heiden, "Convective heat losses in pulse tube coolers: effect of pulse tube inclination," *Cryocoolers 9*, Plenum Publishers, New York (1997), pp. 393-402.
2. Ross, Ronald G., and Dean L. Johnson. "Effect of gravity orientation on the thermal performance of Stirling-type pulse tube cryocoolers," *Cryogenics,* vol. 44, no. 6 (2004), pp. 403-408.
3. Shiraishi, M., Takamatsu, K., Murakami, M., & Nakano, A., "Dependence of convective secondary flow on inclination angle in an inclined pulse tube refrigerator revealed by visualization," *Cryogenics*, vol. 44, no. 2 (2004), pp. 101-107.
4. Swift, G.W. and Backhaus, S., "Why high-frequency pulse tubes can be tipped," *Cryocoolers 16*, ICC Press, Boulder, CO (2011), pp. 183-192.
5. Swift, G.W. and Backhaus, S., "The pulse tube and the pendulum," *Journal of the Acoustical Society of America*, vol. 126, no. 5 (2009), pp. 2273-2284.
6. Berryhill, A. and Spoor, P.S., "High-frequency pulse tubes can't always be tipped," *Advances in Cryogenic Engineering*, vol. 1434, (2012), pp. 1593-1599.
7. Taylor, R.P., "Development and Experimental Validation of a Pulse-Tube Design Tool Using Computational Fluid Dynamics," PhD thesis, The University of Wisconsin-Madison, 2009.
8. Taylor, R.P., Nellis, G. F., and Klein, S. A., "Optimal pulse tube design using computational fluid dynamics," *Advances in Cryogenic Engineering* (J. G. Weisand, I., ed.), American Institute of Physics, vol. 53B (2007), pp. 1445-1451.
9. Mulcahey, T.I., "Convective Instability of Oscillatory Flow in Pulse Tube Cryocoolers due to Asymmetric Gravitational Body Force," PhD thesis, Georgia Institute of Technology, (2014).
10. Mulcahey, T.I., Conrad, T.J., Ghiaasiaan, S.M., and Pathak, M.G., "Investigation of gravitational effects in pulse tube cryocoolers using 3-D CFD," *Advances in Cryogenic Engineering*: *Transactions of the Cryogenic Engineering Conference - CEC* (II, J. G. W., ed.), vol. 59, (2013).
11. Mulcahey, T. I., Conrad, T. J., and Ghiaasiaan, S. M., "CFD modeling of tilt induced cooling losses in inertance tube pulse tube cryocoolers," *Cryocoolers 17*, ICC Press, Boulder, CO (2012), pp. 143-150.

12. Mulcahey T.I., Taylor R.P., Ghiaasiaan S.M., Kirkconnell C.S., Pathak M.G., "Parametric Numerical Study of Off-Axis Pulse Tube Losses," *Cryocoolers 18*, ICC Press, Boulder, CO (2014), pp. 253-261.

13. ANSYS, ANSYS FLUENT User's Guide. No. Release 14.5, Canonsburg, PA 15317: Southpointe, (2012).

14. Lemmon, E.W. and Huber, M.L., REFPROP: NIST Materials Reference Properties Database: Version 9.1. NIST, (2013).

15. Cha, J.S., Ghiaasiaan, S.M., and Kirkconnell, C.S., "Measurement of anisotropic hydrodynamic parameters of pulse tube or Stirling cryocooler regenerators," *Advances in Cryogenic Engineering,* Vol. 51, Amer. Institute of Physics, Melville, NY (2006), pp. 1911-1918.

16. Akhavan, R., Kamm, R. D., and Shapiro, A. H., "An investigation of transition to turbulence in bounded oscillatory stokes flows part 1: experiments," *J. Fluid Mechanics*, vol. 225, (1991), pp. 395-422.